AGU PUBLICATIONS

Water Resources Research

RESEARCH ARTICLE
10.1002/2014WR016144

A soil moisture accounting-procedure with a Richards' equation-based soil texture-dependent parameterization

Simon A. Mathias[1], Todd H. Skaggs[2], Simon A. Quinn[3], Sorcha N. C. Egan[1], Lucy E. Finch[1], and Corinne D. Oldham[1]

[1]Department of Earth Sciences, Durham University, Durham, UK, [2]USDA-ARS, US Salinity Laboratory, Riverside, California, USA, [3]AMEC Environment & Infrastructure, London, UK

Key Points:
- A practical method for estimating vertical percolation using soil texture data
- Percolation rates are consistent with those predicted by Richards' equation
- Vertical percolation rates are studied for a broad set of texture classes

Correspondence to:
S. A. Mathias,
s.a.mathias@durham.ac.uk

Citation:
Mathias, S. A., T. H. Skaggs, S. A. Quinn, S. N. C. Egan, L. E. Finch, and C. D. Oldham (2015), A soil moisture accounting-procedure with a Richards' equation-based soil texture-dependent parameterization, *Water Resour. Res.*, *51*, 506–523, doi:10.1002/2014WR016144.

Received 16 JUL 2014
Accepted 26 NOV 2014
Accepted article online 5 DEC 2014
Published online 23 JAN 2015

Abstract Given a time series of potential evapotranspiration and rainfall data, there are at least two approaches for estimating vertical percolation rates. One approach involves solving Richards' equation (RE) with a plant uptake model. An alternative approach involves applying a simple soil moisture accounting procedure (SMAP) based on a set of conceptual stores and conditional statements. It is often desirable to parameterize distributed vertical percolation models using regional soil texture maps. This can be achieved using pedotransfer functions when applying RE. However, robust soil texture based parameterizations for more simple SMAPs have not previously been available. This article presents a new SMAP designed to emulate the response of a one-dimensional homogenous RE model. Model parameters for 231 different soil textures are obtained by calibrating the SMAP model to 20 year time series from equivalent RE model simulations. The results are then validated by comparing to an additional 13 years of simulated RE model data. The resulting work provides a new simple two parameter (% sand and % silt) SMAP, which provides consistent vertical percolation data as compared to RE based models. Results from the 231 numerical simulations are also found to be qualitatively consistent with intuitive ideas concerning soil texture and soil moisture dynamics. Vertical percolation rates are found to be highest in sandy soils. Sandy soils are found to provide less water for evapotranspiration. Surface runoff is found to be more important in soils with high clay content.

1. Introduction

In many hydrological studies, it is common to estimate the vertical percolation rate expected beneath a soil zone. Following rainfall, some water is intercepted by the vegetation canopy and is subsequently evaporated back to the atmosphere. Rainfall that bypasses the canopy either infiltrates the soil or is transported away as surface runoff. Infiltrated water is then abstracted by plant roots or continues to drain beyond the reach of any vegetation. It is this latter quantity that is referred to hereafter as vertical percolation.

The following definitions are also assumed to apply throughout: net rainfall is defined as the amount of rainfall available for infiltration following deduction of losses associated with canopy interception. Potential evapotranspiration is defined as the amount of water that would be abstracted by plant roots in the presence of abundant soil water. Actual evapotranspiration is defined as the amount of water that is expected to be abstracted by plant roots taking into account the limited availability of soil water. The terms potential and actual evapotranspiration are assumed to exclude losses associated with evaporation from the soil surface and vegetation canopy.

Given a time series of potential evapotranspiration and net rainfall, there are at least two different approaches for estimating vertical percolation rates. One approach involves solving the Richards' equation (a mass conservation equation for two-phase flow in porous media where the air phase is assumed inviscid) with plant roots represented as a distributed, pressure-dependent sink term [*Cox et al.*, 1999; *Smith et al.*, 2006; *Simunek et al.*, 2008; *Best et al.*, 2011]. An alternative approach is to adopt a more simple soil moisture accounting procedure (SMAP) based on a sequence of conceptual stores and conditional statements [*Ragab et al.*, 1997; *Evans and Jakeman*, 1998; *Chapman and Malone*, 2002; *Bradford et al.*, 2002; *Croke and Jakeman*, 2004; *Heathcote et al.*, 2004].

The Richards' equation (RE) typically requires six empirical parameters associated with capillary pressure and relative permeability calculation [*van Genuchten*, 1980]. However, much work has been undertaken to develop pedotransfer functions, whereby these parameters can be estimated using soil texture information

(i.e., % sand, % silt, and % clay) [*Schaap et al*., 2001]. In this way, such a system reduces to a two parameter model (note that sand + silt + clay = 100%). A second benefit is the enabling of parameterization via regional-scale soil texture maps [*Miegel et al*., 2013; *Assefa and Woodbury*, 2013; *Marthews et al*., 2014; *Sorensen et al*., 2014].

A disadvantage of RE models is that they require discretization in both space and time, leading to excessive computational requirements for many practical scenarios. Computation times for RE models can be significantly reduced by using coarser discretizations in space. For this reason, the default number of finite difference grid points used for estimating vertical percolation is often just four [*Cox et al*., 1999; *Smith et al*., 2006; *Best et al*., 2011]. However, inadequate grid resolution has been shown to significantly affect simulated outputs [*de Rosnay et al*., 2000; *Carrera-Hernandez et al*., 2012].

In contrast, SMAP models require discretization only in time and are therefore much faster to execute. Furthermore, the required time steps for RE can be very small (minutes or hours), whereas a SMAP can operate with daily or longer time steps. Consequently, in the UK, the Environment Agency tends to instead advocate the use of SMAPs for regional groundwater recharge estimation studies [*Rushton*, 2005; *Quinn et al*., 2012]. However, robust parameterization of SMAPs is much harder to achieve. Two approaches are generally pursued.

One approach involves coupling a SMAP model with some form of routing function so as to estimate a catchment outlet streamflow. The model parameters (both in the routing function and the SMAP) are then obtained by calibration to observed streamflow gauging data [*Wagener et al*., 1999]. In the case where streamflow gauging data are unavailable, regional relationships derived from alternative rainfall-runoff modelling studies can be used [*McIntyre et al*., 2005]. However, a significant issue is that there is often insufficient information content in the gauging data to adequately condition all the parameters of concern [*Beven and Freer*, 2001]. Furthermore, it is difficult to incorporate spatial variations in soil type data, within the catchment being simulated.

Another approach involves imposing a standardized procedure that links SMAP parameters with soil type data. In the UK, the Environment Agency advocate a method based on the FAO56 [*Allen et al*., 1998] method [*Quinn et al*., 2012]. Spatial variations in soil properties are accounted for using submodels within a given catchment. These are linked together using simple network models for surface runoff [*Heathcote et al*., 2004].

An important aspect of the FAO56 method involves assuming that storage capacity available for plant uptake can be found from the equation, $(\theta_{FC}-\theta_{WP})L_r$, where L_r is the rooting depth and θ_{FC} and θ_{WP} are the moisture contents of the soil at field capacity and wilting-point, respectively [*Allen et al*., 1998]. The parameters, θ_{FC} and θ_{WP}, can be estimated directly from soil texture data using pedotransfer functions such as the ROSETTA model in conjunction with empirical equations such as provided by *Twarakavi et al*. [2009]. However, there is no evidence or theoretical basis to assume that water existing below the vertical extent of the root zone, at one point in time, is forever inaccessible to plants.

In this article, we seek to develop a SMAP with a more physically realistic soil texture-based parameterization obtained by calibration to numerical simulation results from an RE model similar to that used within the widely established MOSES [*Smith et al*., 2006] and JULES [*Best et al*., 2011] land atmosphere interaction models.

The outline of the article is as follows. The governing equations for a numerical Richards' equation (RE) model and an appropriate SMAP are presented. A methodology is described to obtain SMAP parameters for different soil textures by calibration to model output from the RE model. Numerical results are then presented and conclusions discussed.

2. Model Development

2.1. The Richards' Equation (RE) Model

The Richards' equation model applied in this study can be described as follows. A one dimensional mass conservation equation for two-phase flow in porous media where the air phase is assumed inviscid takes the form:

$$\frac{\partial\theta}{\partial t}=-\frac{\partial q}{\partial z}-\lambda \tag{1}$$

where θ [−] is volume of water per unit volume of soil, t [T] is time, z [L] is depth below ground surface, λ

$[T^{-1}]$ is a sink term associated with plant uptake of water, and q $[L\ T^{-1}]$ is the volumetric water flux, found from Darcy's law:

$$q=-K\left(\frac{\partial\psi}{\partial z}-1\right) \tag{2}$$

where K $[L\ T^{-1}]$ is the hydraulic conductivity and ψ (L) is the pressure head.

The following relationships of *van Genuchten* [1980] can be used to relate θ and K to ψ:

$$\theta=(\theta_s-\theta_r)S_e+\theta_r \tag{3}$$

$$K=K_sS_e^{\eta}\left[1-\left(1-S_e^{1/m}\right)^m\right]^2 \tag{4}$$

where S_e $[-]$ is referred to as the effective saturation, found from

$$S_e=(1+|\alpha\psi|^n)^{-m} \tag{5}$$

and where θ_s $[-]$and θ_r $[-]$ are the saturated and residual moisture contents, respectively, K_s $[L\ T^{-1}]$ is the saturated hydraulic conductivity, m $[-]$ is an exponent that relates to n $[-]$ via the relationship $m=1-1/n$, α $[L^{-1}]$ is the reciprocal of a reference state pressure head and η $[-]$ and n $[-]$ are empirical exponents.

The plant uptake term, λ, is obtained using an estimate of potential evapotranspiration (excluding losses associated with evaporation from the soil surface and vegetation canopy), E_p $[L\ T^{-1}]$, in conjunction with an exponential root distribution function, f_1, and the plant stress function of *Feddes et al.* [1976], f_2, such that it can be said that

$$\lambda=f_1(z)f_2(\psi)E_p \tag{6}$$

where

$$f_1(z)=\begin{cases}\dfrac{a}{L_r}\left[\dfrac{\exp(-a)-\exp(-az/L_r)}{(1+a)\exp(-a)-1}\right], & 0\le z\le L_r\\ 0, & z>L_r\end{cases} \tag{7}$$

and [*Feddes et al.*, 1976]

$$f_2(\psi)=\begin{cases}0, & \psi\ge\psi_a\\ 1, & \psi_a>\psi>\psi_d\\ 1-\dfrac{\psi-\psi_d}{\psi_w-\psi_d}, & \psi_d\ge\psi\ge\psi_w\\ 0, & \psi<\psi_w\end{cases} \tag{8}$$

where L_r $[L]$ is the depth of the root zone, a $[-]$ is a parameter that defines how fast the root distribution declines with depth (note that as $a\to 0$, the root distribution approaches a linear function with depth) and ψ_a $[L]$, ψ_d $[L]$, and ψ_w $[L]$ are critical pressure heads associated with anaerobiosis, soil water-limited evapotranspiration, and plant wilting, respectively. Following *Feddes et al.* [1976], these latter three parameters are set to -0.05, -4, and -150 m, respectively. Values of L_r and a are assumed to be 1 and 2 m, respectively for the remainder of the study.

Note that

$$\int_0^{L_r} f_1\,dz=1 \tag{9}$$

such that actual evapotranspiration (excluding losses associated with evaporation from the soil surface and vegetation canopy), E_a $[L\ T^{-1}]$, can be found from

$$E_a = \int_0^{L_r} \lambda \mathrm{d}z \tag{10}$$

Also note that the potential evapotranspiration rate is dependent on plant physiology and a range of meteorological variables including wind speed, humidity, temperature, and radiation. In contrast, the ratio of actual to potential evapotranspiration is assumed to be dependent only on the physiology of the plant and the soil water content.

The initial and boundary conditions are defined as follows:

$$\begin{aligned} \psi &= z - z_{wt}, \quad 0 \le z \le L, \quad t = 0 \\ q &= q_i, \quad z = 0, \quad t > 0 \\ q &= K(\psi), \quad z = L, \quad t > 0 \end{aligned} \tag{11}$$

where L is the depth of soil at which a gravity drainage boundary is imposed, $z_{wt} > L$ [L] is the location of a hypothetical water table from which an initial hydrostatic profile is defined, and q_i [$L\ T^{-1}$] is the infiltration flux, applied at the soil surface boundary, defined as

$$q_i = \begin{cases} q_r, & q_r \le q_p \\ \\ q_p, & q_r > q_p \end{cases} \tag{12}$$

where q_r [$L\ T^{-1}$] is the net rainfall rate (following deduction of losses associated with canopy interception) and q_p [$L\ T^{-1}$] is the flux one would expect when the soil surface is ponded, found from

$$q_p = \left[-K \left(\frac{\partial \psi}{\partial z} - 1 \right) \right]_{z=0, S_e = 0.999} \tag{13}$$

Note that this expression is evaluated with ψ at $z = 0$ fixed such that $S_e = 0.999$ (also note that setting $\psi = 0$ can lead to numerical convergence problems).

The storage water level within the system, Θ [L], can be obtained from the integral

$$\Theta = \int_0^{L} \theta \mathrm{d}z \tag{14}$$

The integrals in equations (10) and (14) are evaluated numerically using trapezoidal integration.

The resulting rates of vertical percolation, q_{vp} [$L\ T^{-1}$], and surface runoff, q_{ro} [$L\ T^{-1}$], are calculated from

$$q_{vp} = q(z = L) \tag{15}$$

$$q_{ro} = q_r - q_i \tag{16}$$

Following *Tocci et al*. [1997], the above set of equations are discretized vertically in space using finite differences, and the resulting set of ordinary differential equations (ODE), with respect to time, solved using method of lines, with ψ selected as the primary dependent variable. Note that by applying a combination of the product rule and the chain rule, the temporal derivative of θ in equation (1) can be written in terms of a temporal derivative of ψ as follows:

$$\frac{\partial \theta}{\partial t} = \left[(\theta_s - \theta_r) \frac{\partial S_e}{\partial \psi} + \theta \rho g (c_r + c_w) \right] \frac{\partial \psi}{\partial t} \tag{17}$$

where ρ [$M\ L^{-3}$] is water density, g [$L\ T^{-2}$] is gravity and c_r [$M^{-1}\ L\ T^2$] and c_w [$M^{-1}\ L\ T^2$] are the compressibilities of soil and water, respectively. The term $\rho g(c_r + c_w)$ is taken to be 9.81×10^{-7} m^{-1} throughout, which is negligibly small. The $\partial S_e / \partial \psi$ term is obtained by analytically differentiating equation (5).

Following *Mathias et al*. [2006, 2008], *Ireson et al*. [2009], and *Ireson and Butler* [2013], the resulting set of ordinary differential equations are solved using MATLAB's ODE solver, ODE15s, which is a variable order solver particularly suitable for solving stiff sets of ODEs [*Shampine and Reichelt* 1997]. ODE15s uses an

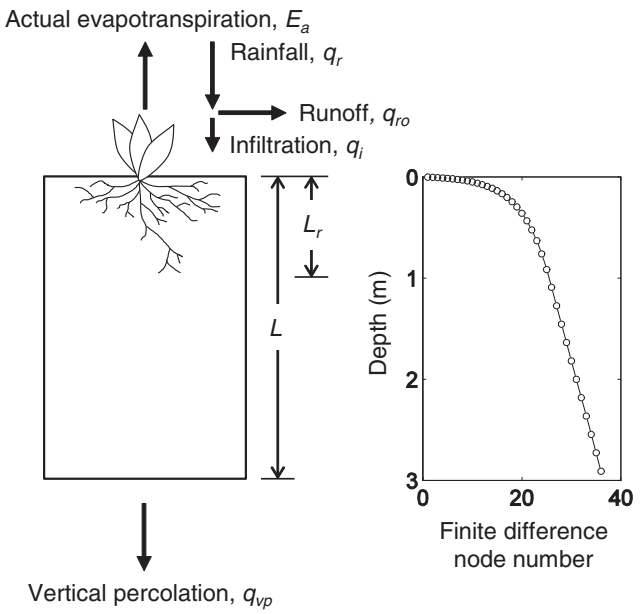

Figure 1. A schematic diagram of the setup used for the Richards' equation (RE) model. Note that the rainfall is a net rainfall following deduction associated with canopy interception losses. Similarly, the calculated actual evapotranspiration does not include ground surface and plant canopy evaporation.

adaptive time stepping scheme to provide a solution at each node for each day of the time series studied. Consequently, a time step for the numerical scheme does not need to be specified a priori.

The finite difference method is applied in a block-centered formulation such that ψ is solved at a set of internal spatial nodes. Node spacing expands logarithmically from 0.0022 m at the surface to 0.1818 m at 1 m depth. Nodes are then equally spaced between 1 and 3 m depth at a spacing of 0.1818 m. A total of 36 nodes are solved for. The fine grid spacing at the surface is needed to accommodate the sharply changing boundary flux due to the daily rainfall data. The uniform spacing in the lower region of the model is needed to adequately resolve the location of the zero-flux-plane, described further in subsection 3.4.

A schematic diagram illustrating the key features of the model setup described above is provided in Figure 1. The model is designed to emulate the default settings generally applied when using the regional-scale modeling packages, JULES, and MOSES. However, the current scheme improves on JULES and MOSES in at least three respects. First, the current scheme uses an adaptive time-stepping scheme as opposed to a constant time step. Second, the spatial scheme involves solving for 36 spatial points as opposed to just four, enabling the model to better capture the dynamics of the zero-flux-plane. Third, the plant uptake model assumes that the local ratio of actual to potential evapotranspiration is a linear function of pressure head as opposed to a linear function of moisture content. In this way, the model is better able to represent how soil texture affects the ability of plant roots to extract their required water.

2.2. The Simplified Soil Moisture Accounting Procedure (SMAP)

The governing equations concerning the simplified soil moisture accounting procedure (SMAP), designed to emulate the Richards' equation (RE) model described above, can be written as follows. First consider the integrated mass conservation statement:

$$\frac{d\Theta}{dt} = q_r - q_{ro} - q_d - E_a \tag{18}$$

where Θ, q_{ro}, and E_a are as previously defined and q_d [$L\ T^{-1}$] is the drainage rate at some intermediate depth within the soil column (i.e., some $z < L$).

In this simplified model, the rate of surface runoff, q_{ro}, is found from

$$q_{ro} = \begin{cases} q_r - q_{ic}, & q_r \geq q_{ic} \\ 0, & q_r < q_{ic} \end{cases} \tag{19}$$

where q_{ic} [$L\ T^{-1}$] is an assumed constant infiltration capacity of the soil.

The drainage rate, q_d [$L\ T^{-1}$], is assumed to be found from

$$q_d = K(\hat{S}_e) \tag{20}$$

where K is found from equation (4) and $\hat{S}_e$ [−] is an upscaled effective saturation, assumed to be found from

$$\hat{S}_e = \frac{\Theta - \Theta_w}{\Theta_{pu}} \tag{21}$$

where Θ_w [L] is the depth of water at which plant wilting occurs and Θ_{pu} [L] is the storage capacity available for plant uptake.

The actual evapotranspiration, E_a, is found from

$$E_a = f_2(\hat{\psi})E_p \tag{22}$$

where E_p is as defined earlier, f_2 is found from the *Feddes et al*. [1976] plant stress function (equation (8)) and $\hat{\psi}$ [L] is an upscaled pressure head. Considering equation (5), $\hat{\psi}$ can be found from

$$\hat{\psi} = -\alpha^{-1}\left(\hat{S}_e^{-1/m} - 1\right)^{1/n} \tag{23}$$

To take into account the additional attenuation that occurs as water travels from the zero-flux-plane to the base of the soil column, the vertical percolation flux, q_{vp}, is calculated from the linear reservoir equation

$$\frac{dq_{vp}}{dt} = \frac{q_d - q_{vp}}{T_r} \tag{24}$$

where T_r [T] is an empirical residence time.

The above set of equations can be implemented using an Euler explicit time-stepping scheme. In this study, a uniform time step of 1 day is used throughout, to suit the daily nature of the rainfall data applied.

2.3. Relating the SMAP Parameters to Soil Texture

In addition to parameters associated with the *van Genuchten* [1980] model and the *Feddes et al*. [1976] plant stress function, the proposed simplified soil moisture accounting procedure (SMAP) above has four empirical parameters: the infiltration capacity, q_{ic}; the storage capacity available for plant uptake, Θ_{pu}; the residence time of the linear reservoir, T_r; and the depth of water at which plant wilting occurs, Θ_w. These four parameters are obtained by calibrating the SMAP model to data generated by the Richards' equation (RE) model described above.

Note that we are not advocating the RE model presented in this article as a panacea for percolation modeling. Notwithstanding the limitations of the Richards' equation itself, the conceptual model described in subsection 2.1 is limited to a one-dimensional homogenous single porosity soil column. In this way, the model is unable to take into account multiscale heterogeneity, the effects of lateral flow within the unsaturated zone and the importance of preferential flow in dual-porosity environments (consider the discussion provided by *Marthews et al*. [2014]).

However, the RE model described in subsection 2.1 is very similar to the default mode typically used in regional-scale land-atmosphere interaction models (JULES, MOSES etc.). Furthermore, in conjunction with the ROSETTA model, the RE model provides a direct link between soil texture data and vertical percolation estimation. The purpose of this article is to provide a methodology for applying an alternative, more simple SMAP for estimating vertical percolation of a similar nature.

To this end, the RE model is run for 231 different soil textures for the period of 1961–1998 using daily rainfall data and monthly potential evapotranspiration data from the Theale gauging station in the Kennet valley, Berkshire, UK. The local region has a maritime climate with an average annual rainfall of 670 mm [*Bradford et al*., 2002].

The meteorological data were extracted from the UK regionalization database previously developed and presented by *Young* [2000, 2006]. The rainfall data were derived using the UK Meteorological Office daily rainfall library and a modified version of the Triangular Planes interpolation methodology of *Jones* [1983] and *Young* [2000]. Time series of Penman Monteith reference crop potential evapotranspiration was

estimated using data from the Meteorological Office Rainfall and Evaporation Calculation System (MORECS) *Hough* [1995].

The 231 soil textures are chosen such as to provide a set of nodes across the soil texture triangle with equal spacings of 5% sand, 5% silt, and 5% clay. A set of *van Genuchten* [1980] parameters $(\theta_r, \theta_s, \alpha, n, K_s, \eta)$ are obtained for each soil texture using the ROSETTA pedotransfer function [*Schaap et al*., 2001].

The resulting RE model data are split into three periods. The period of 1961–1964 is used for a warm-up period to eliminate problems associated with initial conditions. The period of 1964–1984 is used for calibration. The period of 1984–1998 is set aside for a validation period to assess the extent to which the SMAP model predictions match those of the RE model.

Because, the amount of runoff (q_{ro}) generated by the SMAP model is dependent only on the net rainfall (q_r), the infiltration capacity parameter, q_{ic}, can be obtained independently of the other three parameters. Consequently, a value of q_{ic}, for each soil texture, is obtained by matching the total q_{ro} generated during the calibration period by equation (19) with that generated by the equivalent RE model. The matching is achieved using MATLAB's optimization function, FMINSEARCH.

Although Θ_w affects the magnitude of the storage level (Θ), from the perspective of vertical percolation (q_{vp}), the value of Θ_w is an arbitrary reference point. Therefore, when calibrating the SMAP model to q_{vp} data, it is possible to treat Θ_{pu} and T_r independently of Θ_w.

This is achieved by first setting Θ_w to zero. With q_{ic} and Θ_w set a priori, values of Θ_{pu} and T_r are obtained for each soil texture by maximizing the *Nash and Sutcliffe* [1970] efficiency (NSE) criterion (again using FMINSEARCH) whereby

$$\mathrm{NSE}=1-\frac{\sum_{i=1}^{N}(o_i-m_i)^2}{\sum_{i=1}^{N}(o_i-\overline{o_i})^2} \tag{25}$$

and N is the number of data points, o_i are the observed data, m_i are the modeled data, and $\overline{o_i}$ is the mean of the observed data. In this case, the data are values of q_{vp}, the RE model output is treated as the observed data and the SMAP model output is treated as the modeled data. Negative NSE implies that the model is worse than the mean at representing the observed data. The closer NSE is to 1 the better the model.

Once optimal values of q_{ic}, Θ_{pu}, and T_r have been obtained, a value of Θ_w is chosen such that the Θ data from the RE model and the SMAP model have the same mean values over the calibration period.

The advantages of taking such a sequential approach to calibration are as follows: all SMAP models produce the same quantity of runoff during the calibration period as their RE model counterparts. All SMAP models have the same mean storage level during the calibration period as their RE model counterparts. The calibration of the SMAP model to the q_{vp} data only involves two free parameters enabling the use of sophisticated local optimization routines such as FMINSEARCH.

3. Results and Discussion

3.1. A Study of Three Different Soil Textures

Figures 2–4 show simulated output for three very different soil-types, a sandy soil, a clay soil, and a silty soil, respectively. Only the years 1988–1995 (from the validation period) are shown for clarity. Note that the black lines are from the Richards' equation (RE) model and the red lines are from the simplified soil moisture accounting procedure (SMAP).

Surface runoff (q_{ro}) is only observed in the clay soil (Figure 3a). The other two soils are seen to accommodate all the incoming rainfall (compare Figures 2a and 4a). Even for the clay soil, there are very few runoff events. This is largely due to the use of daily sampling of the rainfall data, which smooths the much higher intensity subdaily events that may have occurred. The calibrated SMAP model can be seen to accurately approximate the timing for all of the larger runoff events (where $q_{ro} > 1$ mm/d) although the magnitudes are not quite right. However, the implications of this discrepancy on the approximation of vertical percolation (q_{vp}) are not that significant because runoff is found to represent $<1\%$ of total net rainfall (q_r) for all soil textures, in this context (Figure 5b).

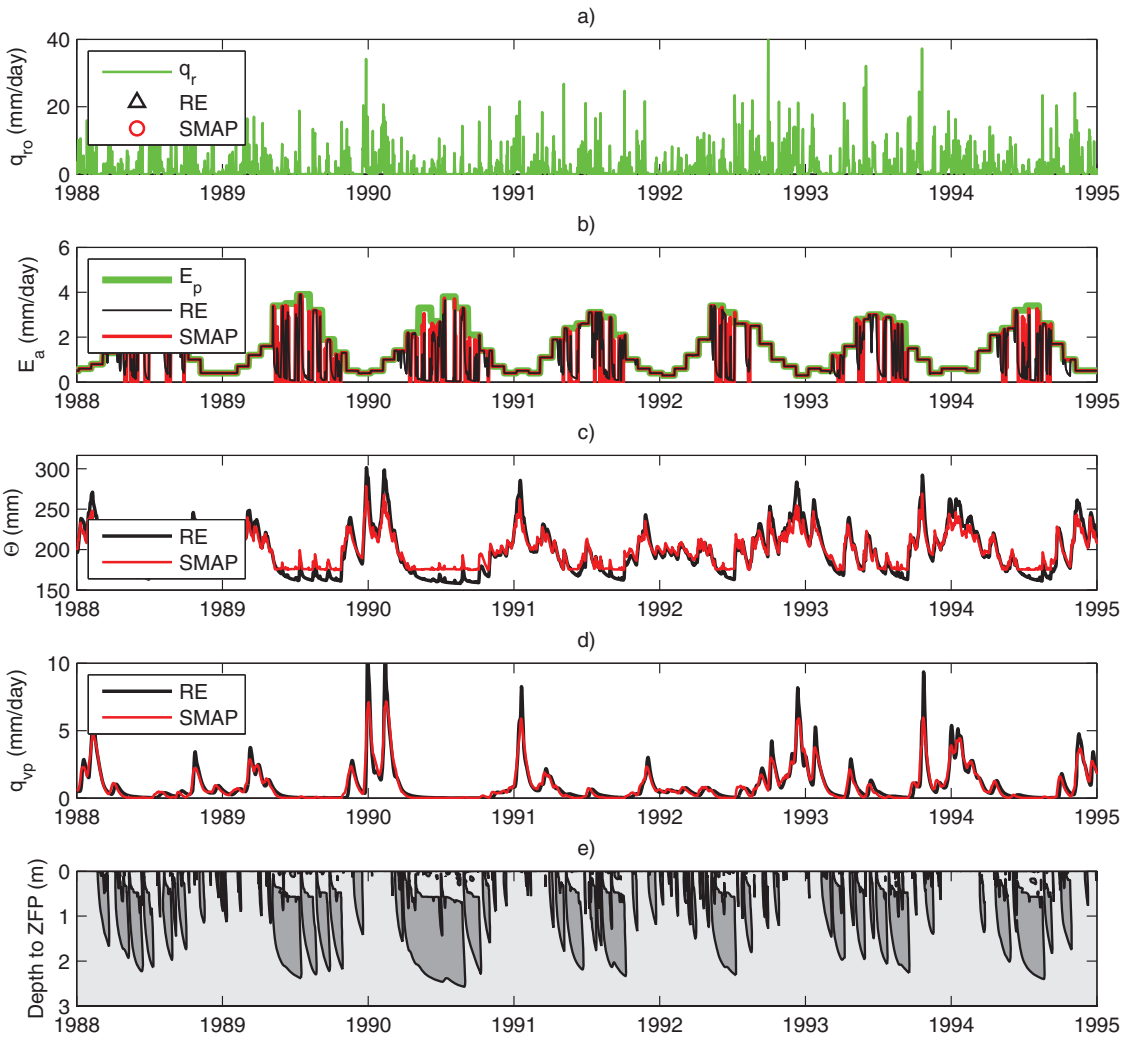

Figure 2. Results for a sandy soil column with 90% sand, 5% silt, and 5% clay, using both the Richards' equation (RE) model (in black) and the simple soil moisture accounting procedure (SMAP) model (in red). (a) Plot of simulated surface runoff (q_{ro}) alongside the imposed net rainfall (q_r) time series (in green). (b) Plot of simulated actual evapotranspiration (E_a) alongside the imposed potential evapotranspiration (E_p) time series (in green). (c) Plot of simulated storage water level (Θ). (d) Plot of simulated vertical percolation (q_{vp}). (e) Plot of simulated depth to the zero-flux-plane (ZFP) using the RE model. Darker-shaded and lighter-shaded regions denote areas of upward and downward flow, respectively. Note that for this soil, there is no surface runoff during the period presented.

The sandy soil is frequently unable to supply actual evapotranspiration (E_a) at the potential rate (E_p) (Figure 2b). The reason for this is that the permeability of sand is very high and therefore rainfall quickly drains through the system and is then unavailable for evapotranspiration. The clay soil is able to provide more of the E_p although each summer there are several episodes where E_a becomes limited (Figure 3b). The situation is more favorable (from an E_a perspective) for the silty soil where it can be seen to provide E_p for most of the time except during the summers of 1989 and 1990 and a few small episodes in the summers of 1991, 1992, and 1994 (Figure 4b). Similar results are also observed for the calibrated SMAP model although the SMAP model has a tendency to overestimate E_a (as compared to the RE model).

The storage level (Θ) in the sandy soil ranges from 150 to 300 mm, and for both the clay and the silty soils, from 1000 to 1400 mm (compare Figures 2c, 3c, and 4c). This difference in ranges is largely due to differences in θ_r and θ_s. It is also evident that the sand storage shows faster recessions following individual rainfall events, probably due to its higher permeability. The calibrated SMAP model exhibits very similar characteristics in this respect. However, for the sandy soil (Figure 2c), the SMAP model overestimates Θ for the lower values of Θ (as compared to the RE model). The reason for this is that the calibration is based on the q_{vp} data and, for the sandy soil, the rate of q_{vp} is largely insensitive to Θ at low q_{vp} rates.

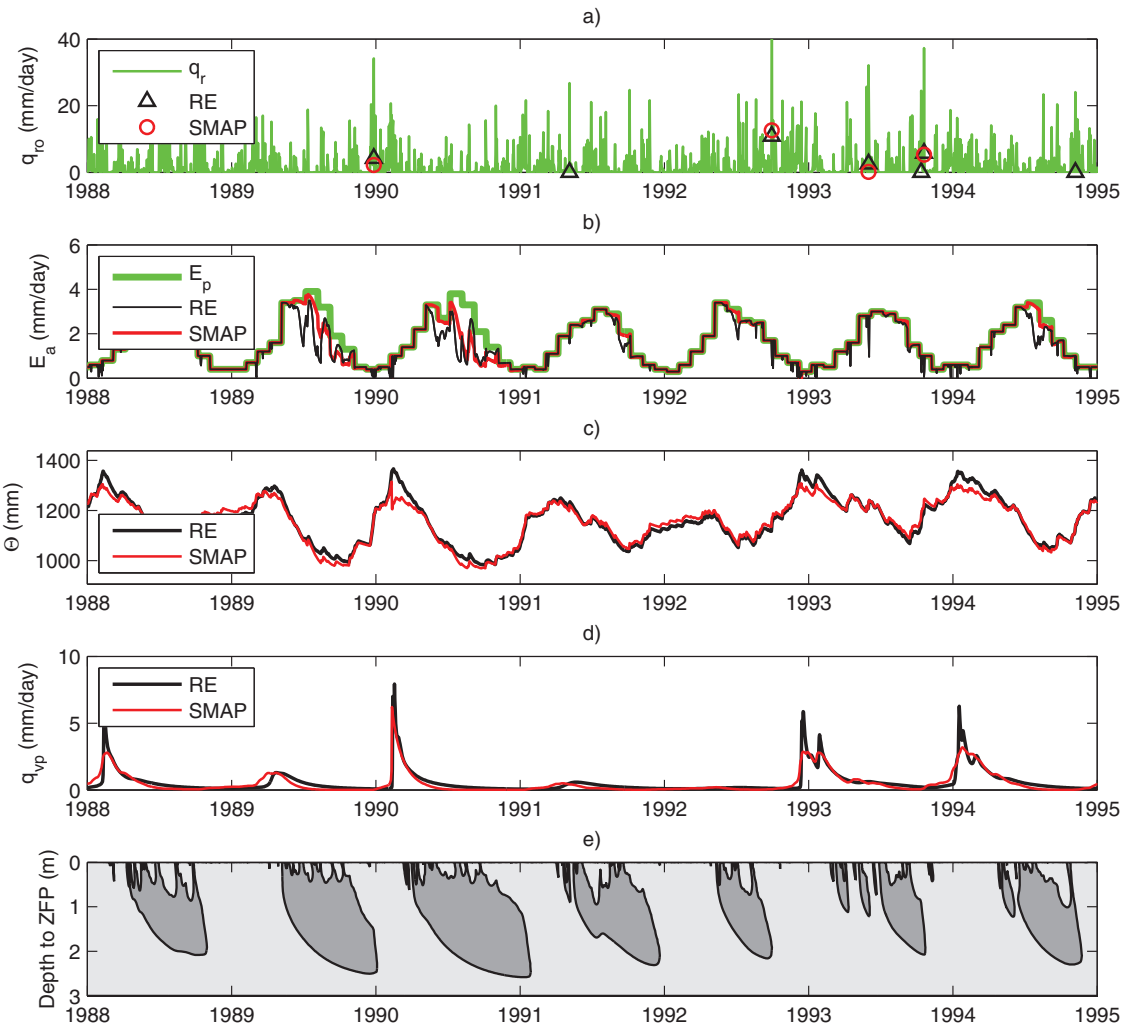

Figure 3. Results for a clay soil column with 30% sand, 5% silt, and 65% clay, using both the Richards' equation (RE) model (in black) and the simple soil moisture accounting procedure (SMAP) model (in red). (a) Plot of simulated surface runoff (q_{ro}) alongside the imposed net rainfall (q_r) time series (in green). (b) Plot of simulated actual evapotranspiration (E_a) alongside the imposed potential evapotranspiration (E_p) time series (in green). (c) Plot of simulated storage water level (Θ). (d) Plot of simulated vertical percolation (q_{vp}). (e) Plot of simulated depth to the zero-flux-plane (ZFP) using the RE model. Darker-shaded and lighter-shaded regions denote areas of upward and downward flow, respectively.

The sandy soil exhibits a fast reacting response to rainfall events with very short recession periods leading to many episodes of zero vertical percolation (q_{vp}) (Figure 2d). The q_{vp} response for the clay soil is much more seasonal (Figure 3d). The q_{vp} rates in the silty soil are generally much lower and smoother with moderate drainage rates observable throughout the summer periods (Figure 4d). The higher peak flows seen in the clay soil (as compared to the silt soil) are due to the 30% sand contribution and also the fact that E_a is less (as compared to the silty soil) (compare Figures 3d and 4d). Generally, the SMAP model is seen to provide a good approximation for q_{vp} although there is a tendency to underestimate the peak values (as compared to the RE model). In most cases, this is due to the SMAP model overestimating E_a (as compared to the RE model), and consequently there is not enough water available to generate the slightly higher q_{vp} events.

3.2. The Global Response of the Richards' Equation (RE) Model

Notwithstanding the main focus of the paper, which is to develop a SMAP to emulate the RE model in terms of vertical percolation forecasting, given the undertaking of the 231 numerical simulations, it is interesting to study the global response of the RE model to soil texture. Figure 5 summarizes the response of the RE model over the entire textural triangle. These results are based on summations and ranges of the state variables over the period of 1964–1998. The first 3 years are neglected to avoid warm-up issues associated with the hydrostatic initial condition.

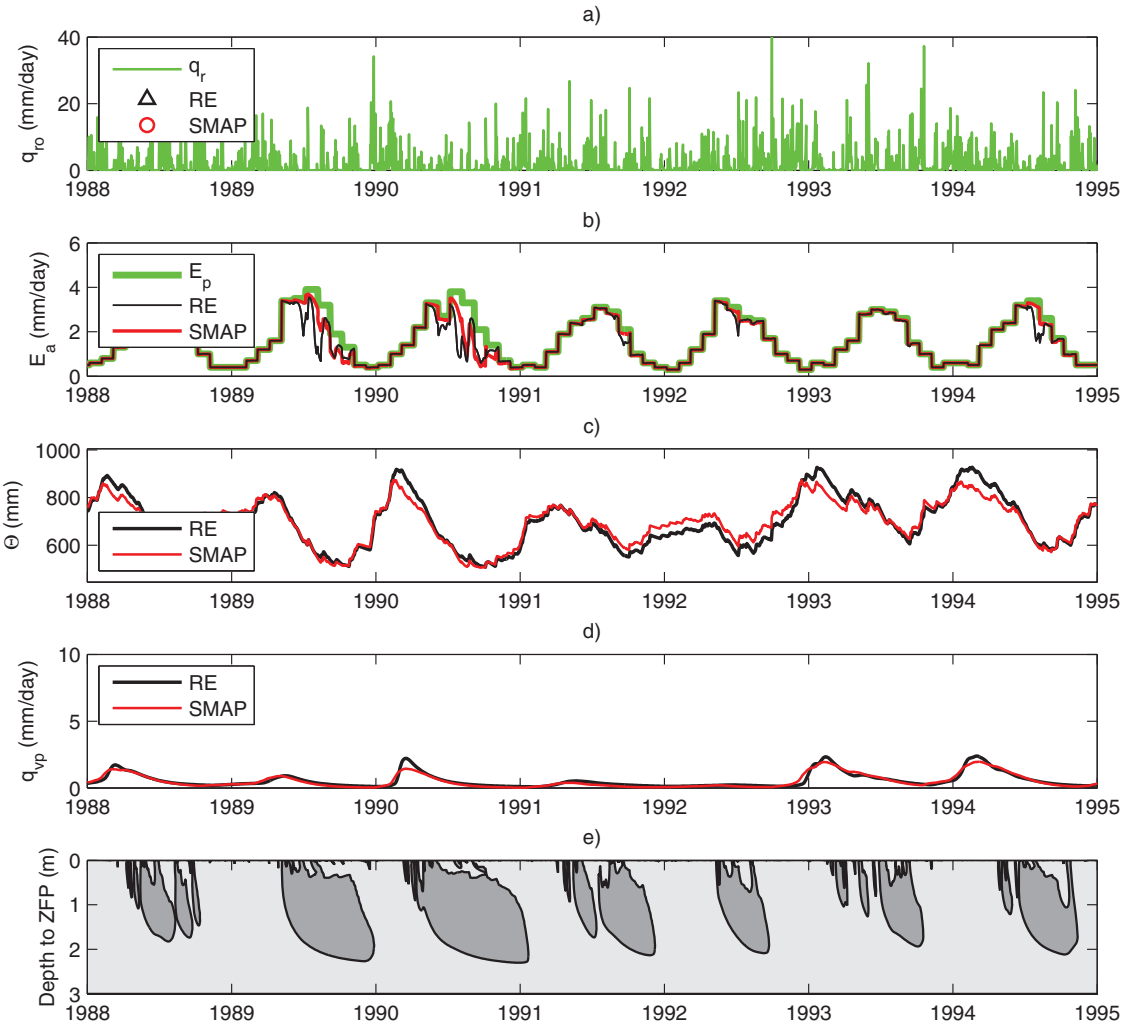

Figure 4. Results for a silty soil column with 5% sand, 90% silt, and 5% clay, using both the Richards' equation (RE) model (in black) and the simple soil moisture accounting procedure (SMAP) model (in red). (a) Plot of simulated surface runoff (q_{ro}) alongside the imposed net rainfall (q_r) time series (in green). (b) Plot of simulated actual evapotranspiration (E_a) alongside the imposed potential evapotranspiration (E_p) time series (in green). (c) Plot of simulated storage water level (Θ). (d) Plot of simulated vertical percolation (q_{vp}). (e) Plot of simulated depth to the zero-flux-plane (ZFP) using the RE model. Darker and lighter shaded regions denote areas of upward and downward flow, respectively. Note that for this soil, there is no surface runoff during the period presented.

It can be seen that over most of the textural triangle, the simulated total actual evapotranspiration (E_a) is between 90% and 94% of the total potential evapotranspiration (E_p) (Figure 5a). However, as the soil becomes progressively sandy, total E_a is less than 80% of the total E_p. The reason is that the permeability of the sand is much higher than the other soils. Consequently, water is passing through the soil columns much faster and has less time available to be accessed by the plant roots.

Runoff (q_{ro}) is seen to only occur in soils with low silt content and less than 50% sand content (Figure 5b). However, total q_{ro} represents less than 1% of total net rainfall (q_r) in all cases. This low figure could be due to the use of daily rainfall data, as discussed above. The highest runoff occurs in soils with 0% silt and around 70% clay (with around 30% sand).

It can be seen that total vertical percolation (q_{vp}), represents between 27% and 30% of total q_r for most soil textures (Figure 5c). However, as soil becomes progressively sandy, total q_{vp} increases to over 40% of the total q_r. This is largely due to the reduced E_a associated with these soils, as discussed above.

The range of variation in storage depth of water (Θ), is between 400 and 500 mm for most soils (Figure 5d). But this reduces to below 100 mm for very sandy soils. This is likely to be due to a reduction in the

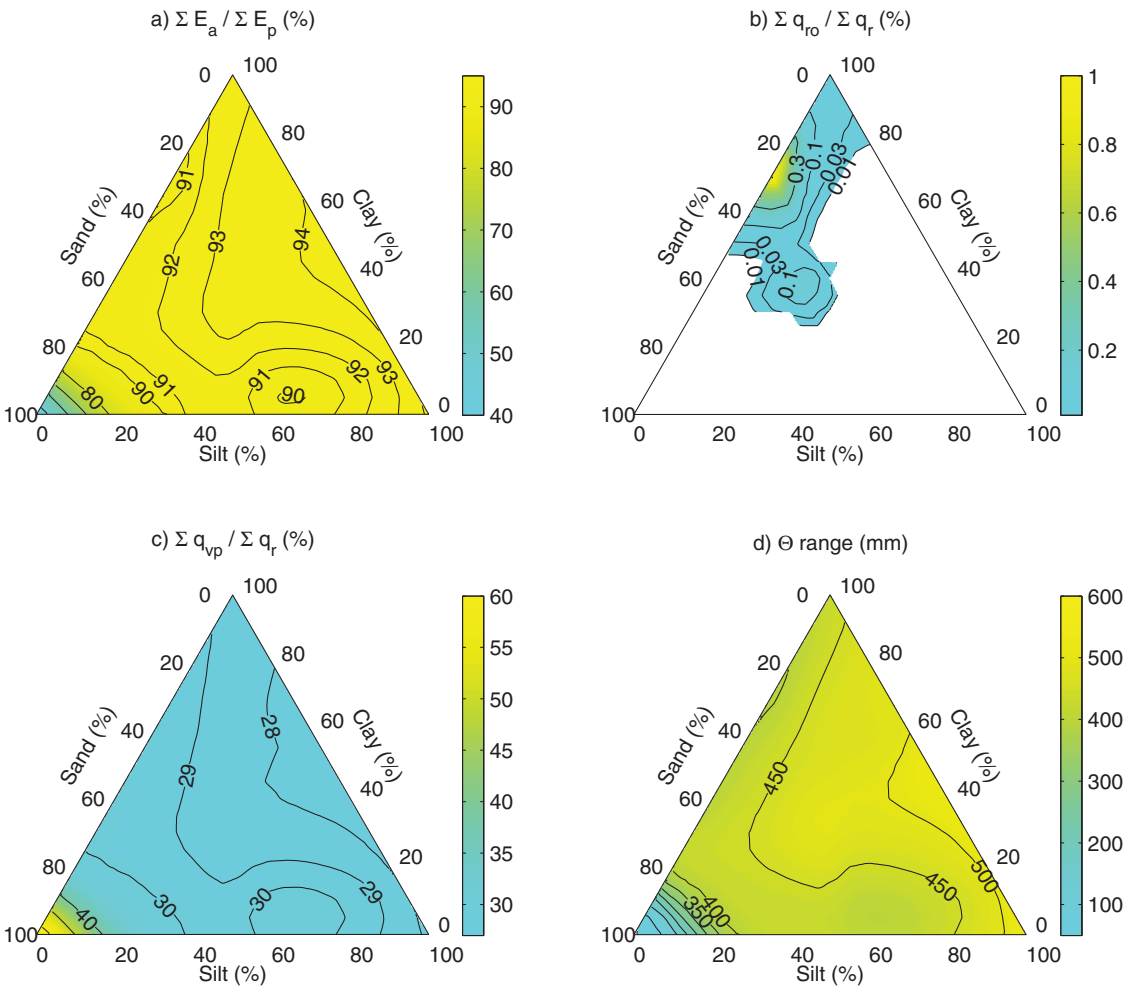

Figure 5. Ternary diagrams illustrating the response of the RE model to soil texture. (a) Total actual evapotranspiration (E_a) as a percentage of total potential evapotranspiration (E_p). (b) Total surface runoff (q_{ro}) as a percentage of total net rainfall (q_r). (c) Total vertical percolation (q_{vp}) as a percentage of total net rainfall (q_r). (d) The difference between the maximum and minimum storage water level (Θ) in mm.

difference between θ_s and θ_r, and also the fact that sandy soils never approach complete saturation due to the larger drainage rates associated with their higher permeabilities.

3.3. The Global Response of the SMAP

The resulting calibrated SMAP parameter distributions across the textural triangles are shown in Figure 6. Figure 6a shows the variation of the infiltration capacity (q_{ic}). The triangle is empty beyond 60 mm/d because this was the maximum rainfall rate experienced during the calibration period. The lower the q_{ic}, the more runoff will occur for a given soil. Soils with high clay content and low silt content are most prone to runoff occurring, as previously observed in Figure 5b.

The silty soils have the largest amounts of storage capacity available for plant uptake (Θ_{pu}), over 700 mm in depth (Figure 6b). The smallest amounts of Θ_{pu}, between 450 and 500 mm, are observed for sandy clay soils with low silt content. Interestingly, pure sand is seen to also have a quantity of Θ_{pu} of over 700 mm, whereas the observed Θ range is less than 100 mm (recall Figure 5d). This implies that the sandy soil columns are always far away from saturation due to their ability to quickly drain any residing water.

The higher the residence time (T_r), the more attenuated the vertical percolation (q_{vp}) is expected to be. Not surprisingly, the largest T_r values are found in the silt corner (Figure 6c). T_r is in excess of 70 days for pure silt. In contrast for pure sand, T_r is less than 10 days. The associated attenuation is inversely proportional to the hydraulic diffusivity of the soil. Hydraulic diffusivity is proportional to permeability and inversely

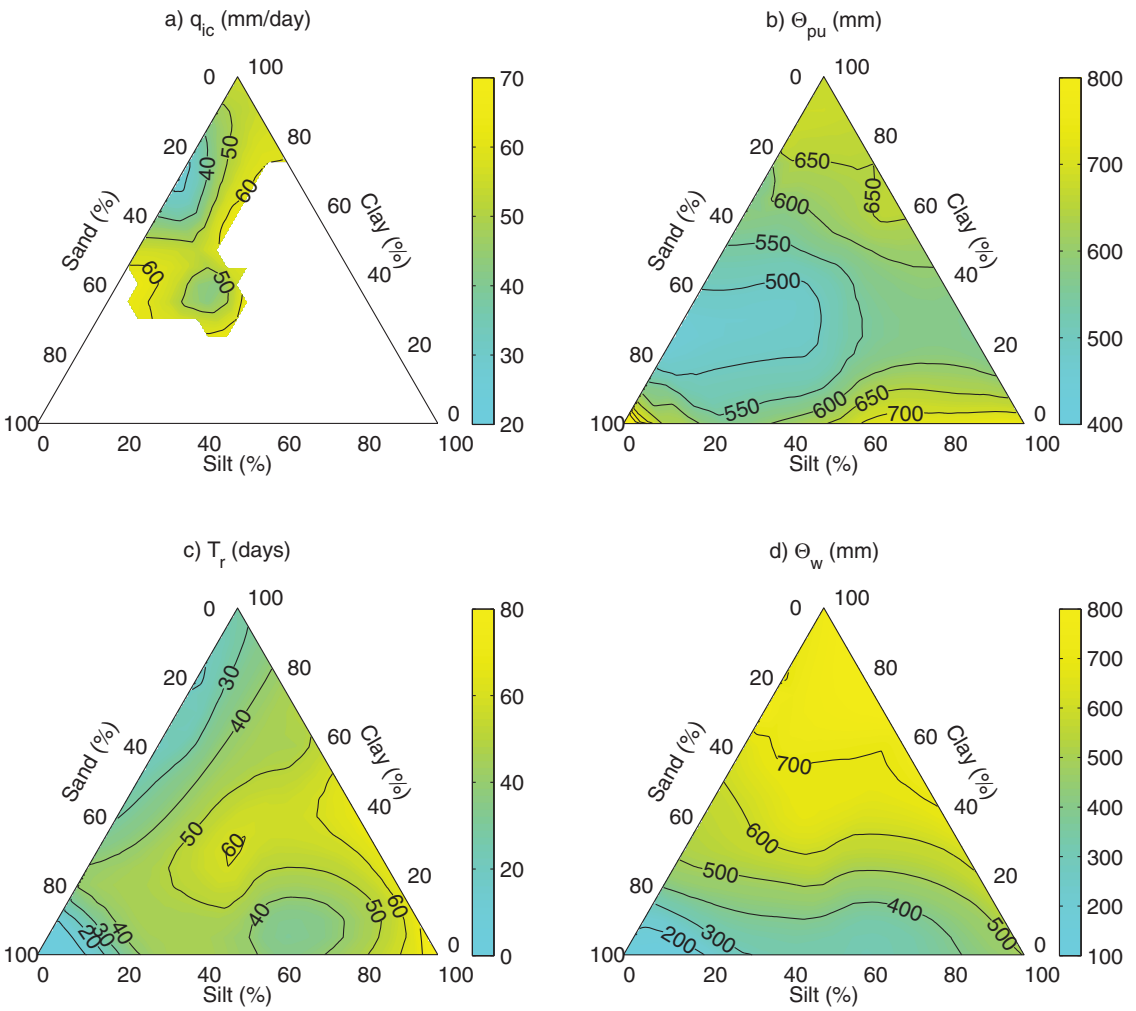

Figure 6. Ternary diagrams illustrating the variation in calibrated SMAP model parameters with soil texture. (a) Infiltration capacity, q_{ic} (mm/d). (b) Storage capacity available for plant uptake, Θ_{pu} (mm). (c) Residence time of the linear reservoir, T_r (days). (d) Depth of water at which plant wilting occurs, Θ_w (mm).

proportional to storage capacity. Sand has a high permeability and a low storage capacity, therefore, a high hydraulic diffusivity and a small residence time. Silt has a moderate permeability but also has a very large storage capacity and therefore a large residence time.

The depth of water storage below which the associated plant wilts (Θ_w) is a measure of the residual water that never drains from the column or is abstracted by plants. The largest values are found in the clay soils (>700 mm) and the lowest in the sandy soils (<200 mm) (Figure 6d). The variation is heavily controlled by the residual moisture content of the soils, θ_r.

Variations in goodness of fit are illustrated, as contour plots of NSE across the textural triangle, in Figure 7. For reference and comparison, the NSE values for the soils presented in Figures 2–4 are given in Table 1 along with optimal values for the four SMAP parameters: Θ_{pu}, Θ_w, T_r, and q_{ic} and the associated ROSETTA model parameters.

Figure 8 shows a cross plot of the SMAP model parameters with themselves and also the *van Genuchten* [1980] parameters. It is clear that the four SMAP model parameters have very little correlation with themselves. This can largely be attributed to the sequential approach to parameter calibration discussed in subsection 2.3.

The Θ_{pu} parameter generally increases with increasing θ_s–θ_r. This is not surprising because the difference, θ_s–θ_r, represents the drainable porosity of the soil column. The highest K_s parameters correspond with the

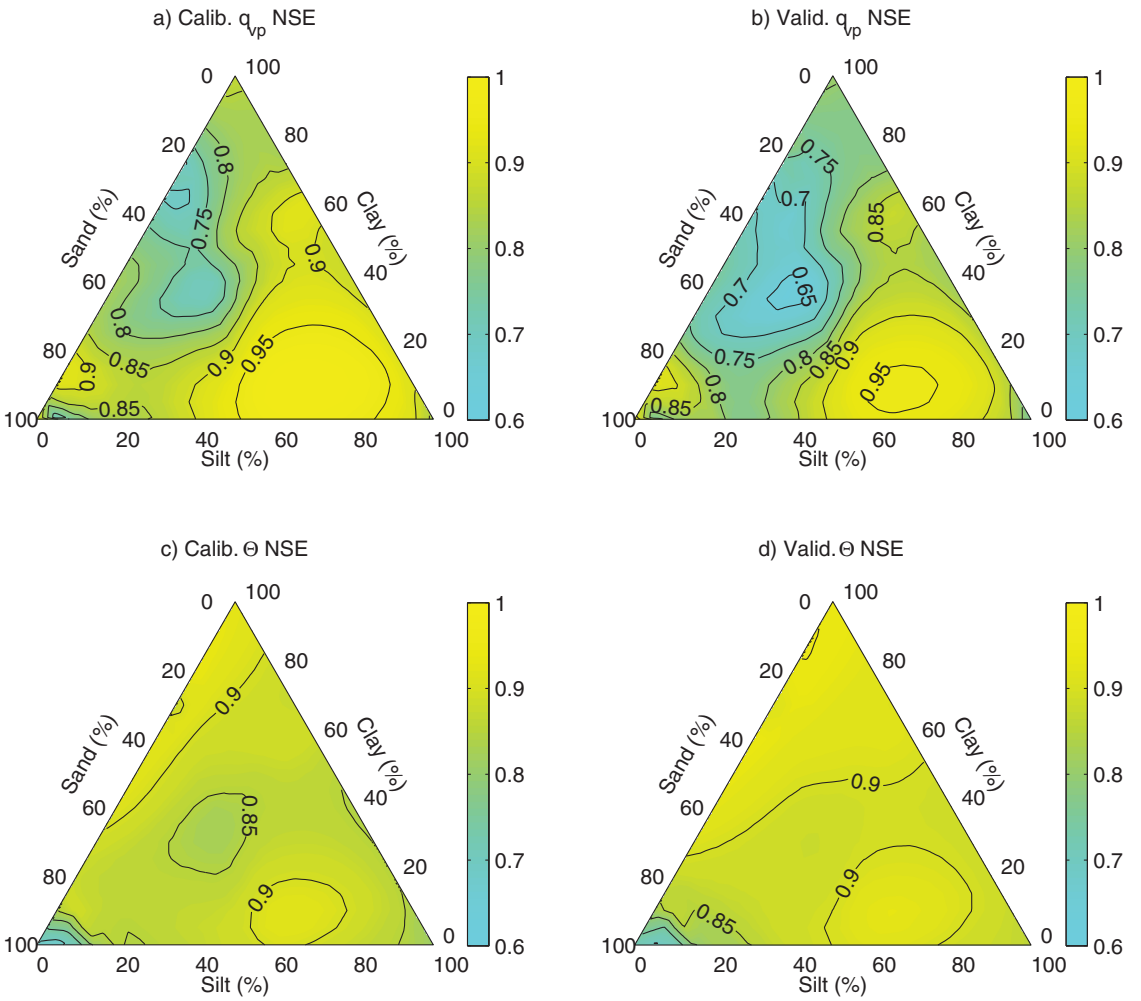

Figure 7. Ternary diagrams illustrating variation in goodness of fit between the RE model and the SMAP model. (a) NSE based on vertical percolation rates (q_{vp}) during calibration period. (b) NSE based on vertical percolation rates (q_{vp}) during validation period. NSE based on storage water level (Θ) during calibration period (Figure 7a). NSE based on storage water level (Θ) during validation period (Figure 7b).

lowest T_r parameter values. However correlation between T_r and K_s is lost once $K_s < 10^{-5}$ m/s. The residence time is likely to be inversely proportional to the hydraulic diffusivity of the system, which in turn will be linearly proportional to K_s. The Θ_w parameter increases with increasing θ_r and decreases with increasing K_s. The

Table 1. *Nash and Sutcliffe* [1970] Efficiency (NSE) Values and Model Parameters Used for the Sandy Soil, Clay Soil, and Silty Soil Models Presented in Figures 2–4, Respectively

	Sandy Soil (Figure 2)	Clay Soil (Figure 3)	Silty Soil (Figure 4)
NSE for vertical percolation during calibration	0.8609	0.6901	0.9318
NSE for vertical percolation during validation	0.8705	0.7107	0.8838
NSE for storage water level during calibration	0.7645	0.9178	0.8511
NSE for storage water level during validation	0.7460	0.9307	0.8808
Infiltration capacity, q_{ic} (mm/d)	N/A	31.98	N/A
Storage capacity available for plant uptake, Θ_{pu} (mm)	600.6	604.2	679.2
Residence time of linear reservoir, T_r (days)	7.349	22.20	60.71
Water level at wilting-point, Θ_w (mm)	174.0	709.2	469.7
Residual moisture content, θ_r (−)	0.0515	0.0961	0.0506
Saturated moisture content, θ_s (−)	0.3769	0.4616	0.5204
Reciprocal of air-entry pressure, α (m^{-1})	3.321	2.711	0.8294
Capillary pressure exponent, n (−)	2.503	1.149	1.649
Saturated hydraulic conductivity, K_s (mm/d)	3220	108.5	405.1
Relative permeability exponent, η (−)	−0.8653	−5.153	0.5452

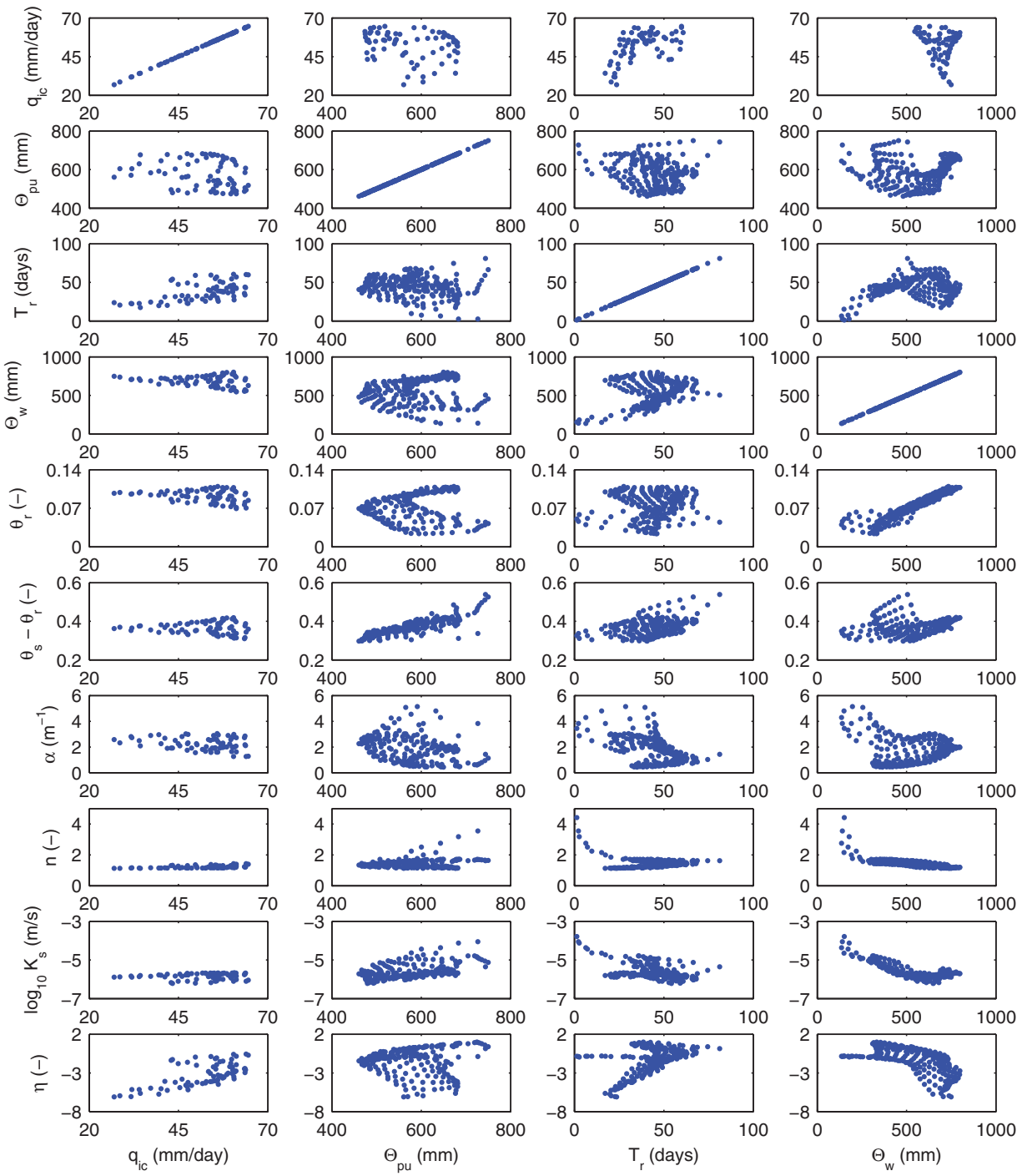

Figure 8. Cross plots of SMAP model parameters with *van Genuchten* [1980] parameters.

reason is that Θ_w is always going to be larger than the $L\theta_r$ product; how much larger is dependent on how permeable the drainable porosity is. There are no apparent correlations for q_{ic} although it is clear that this parameter is only defined where $K_s < 2 \times 10^{-6}$ m/s. For higher permeability soils, surface runoff is less likely to occur.

3.4. The Zero-Flux-Plane (ZFP)

The depth at which the hydraulic gradient is zero (and hence the flow rate is zero) represents a zero-flux-plane (ZFP) [*Wellings and Bell*, 1980]. During winter periods when potential evapotranspiration (E_p) is low,

flow is downward throughout the profiles. As the summer develops, plant roots suck water up. Therefore, in the upper region, water is moving upward, whereas in the lower region, water is moving downward. The interface between these two regions is a ZFP. But during the summer, further rainfall can lead to an additional ZFP due to downward infiltration fluxes from the surface. Eventually, as summer closes, the upward flow region disappears, and flow is downward throughout the profile for the following winter. The cycle then repeats itself during the following year.

Although the SMAP model is unable to provide information about the ZFP, it is interesting to study the ZFP results from the RE model. Figures 2e, 3e, and 4e show the depth to the zero-flux-plane (ZFP) and how this varies with time. The darker-shaded and lighter-shaded regions are areas of upward and downward flow, respectively. Both the clay and silty soils exhibit a similar ZFP pattern as described above. However, the sandy soil exhibits a much less seasonal pattern, with the summer time ZFP frequently broken up by large infiltration events, which reach the base of the column. All three soils produce a continuous net downward flux at the base of the columns throughout the year. Also of interest is that the ZFP is often approaching below 2.5 m from the soil surface. Although the plant roots are limited to the top 1 m, it is clear that they are able to access soil water from much deeper depths.

As mentioned previously, within the FAO56 method [*Allen et al*., 1998], the total available water (TAW) parameter (which is similar to Θ_{pu} in this article) is assumed to be calculated from $(\theta_{FC}-\theta_{WP})L_r$ where L_r [L] is the rooting depth and θ_{FC} [$-$] and θ_{WP} [$-$] are the moisture contents of the soil at field capacity and wilting-point, respectively. But the above results suggest that plant roots are able to access much more water. Our new SMAP model is able to better accommodate this point due to the fact that Θ_{pu} is obtained, for a given soil texture, by direct calibration to the model output from the RE model.

3.5. Some Notes on Bypass Flow

In a recent study, *Sorensen et al*. [2014] applied three different SMAP models and an RE model to four different field sites in the UK. All four models were parameterized a priori using soil type maps of the areas. The models were then assessed in terms of their ability to predict several years of soil water observations from the sites in question. All four models predicted relatively similar soil water responses to the observed data. However, the estimates of vertical percolation were widely varying.

The RE model used by *Sorensen et al*. [2014] was from the JULES package [*Best et al*., 2011]. The three SMAP models applied included FAO56 [*Allen et al*., 1998], the Penman-Grindley (PG) model [*Grindley*, 1967], and SPADE [*Finch*, 2001]. FAO56 assumes that when the storage level (Θ) drops below a given constant, Θ_c, (somewhere between Θ_w and $\Theta_w+\Theta_{pu}$) the ratio of actual to potential evapotranspiration (E_a/E_p) linearly decreases from one to zero as Θ approaches the wilting-point (Θ_w). The PG model is identical to FAO56 except that the E_a/E_p ratio is assumed to reduce to a constant fraction (less than one) when $\Theta_w < \Theta < \Theta_c$. The SPADE model is similar to the PG model except that there are four layers considered such that there are three stepped declines in the ratio E_a/E_p, as described by *Ragab et al*. [1997].

Of particular note is that for all three SMAPs, vertical percolation only occurs when Θ exceeds the storage capacity of the system $(\Theta_w+\Theta_{pu})$. In this way, the system is thought to be at field capacity when $\Theta=\Theta_w+\Theta_{pu}$ [*Ragab et al*., 1997]. Consequently, *Sorensen et al*. [2014] found that the three SMAP models predicted many periods when $q_{vp}=0$, whereas JULES predicted a persistent nonzero q_{vp} throughout the simulation periods. Unfortunately, it is not possible to directly observe q_{vp} in situ without the presence of a lysimeter. Therefore, it is not possible to determine which models were more realistic.

However, the problem of SMAP models predicting zero q_{vp} unless $\Theta > \Theta_w+\Theta_{pu}$ often leads to the unrealistic prediction of summer streamflow recessions that are unreactive to summer-time rainfall events [*Ireson et al*., 2009]. A common solution is to incorporate a bypass term whereby a fraction of the rainfall is assumed not to enter the SMAP and is diverted directly to the routing function or groundwater flow model [*Rushton*, 2005]. Bypass is often treated as a constant fraction of the precipitation and/or assumed to only occur when the precipitation rate exceeds a predetermined threshold [*Rushton*, 2005; *Wagener et al*., 2003; *Ireson et al*., 2009]. Physically, the bypass contribution is thought to represent flow through macropores in the unsaturated zone and/or infiltration excess overland flow [*Wagener et al*., 2003]. In fractured rock systems, the need for bypass flow in SMAP models is widely attributed to flow in fractures within the unsaturated zone [*Rushton*, 2005].

Chapman and Malone [2002] studied the performance of 13 different SMAP models to simulate observed drainage from a 2.4 m deep weighing lysimeter experiment. The lysimeter was filled with a well-drained silt loam overlain by a permanent grass crop. Following calibration to observed soil moisture data, only two of the 13 models were able to provide adequate forecasts of the drainage data. Of note was that both of these models treated bypass flow as a nonlinear function of the storage level (Θ), similar to the SMAP model proposed in subsection 2.2. Similar findings were also observed by *Black et al*. [1969] and *Aston and Dunin* [1977].

Notwithstanding the importance of macropores and fractures, it is interesting to note that in the context of field capacity-based SMAPs, a bypass flow component is required to model a lysimeter of relatively homogenous soil. Relating back to the numerical work presented in subsection 3.1, none of the three examples presented in Figures 2–4 exhibit an obvious field capacity whereby the storage level (Θ_w) reaches some regular maximum level during the winter seasons. In the context of field capacity-based SMAPs, the bulk of the q_{vp} generated by the homogenous single porosity RE models would be attributed to some form of bypass flow. This is not necessary in our new SMAP because, similar to *Chapman and Malone* [2002], q_{vp} is treated as a continuous nonlinear function of Θ_w and the concept of field capacity is not necessarily invoked.

4. Summary and Conclusions

The objective of this study was to develop a simple soil moisture accounting procedure (SMAP) designed to emulate a one-dimensional homogenous Richards' equation (RE) model with a pressure-dependent plant stress function to limit actual evapotranspiration. The advantage of the SMAP is that its model parameters can be calculated using pedotransfer functions such as the ROSETTA model [*Schaap et al*., 2001] while being much more computationally efficient than RE models. A computationally efficient SMAP will be of practical benefit for regional-scale land-atmosphere interaction models, groundwater recharge estimation, and other hydrologic modelling applications where vadose zone water fluxes are important and model complexity and/or long model execution times are a concern.

The SMAP model involves defining an upscaled effective saturation. This is used to calculate an effective pressure head and hydraulic conductivity using the relationships of *van Genuchten* [1980]. The pressure head is used in conjunction with the *Feddes et al*. [1976] plant stress function to calculate actual evapotranspiration. The hydraulic conductivity is used to define how much vertical percolation drains from the SMAP.

Although the SMAP model requires the estimation of at least seven parameters (q_{ic}, Θ_{pu}, T_r, α, n, K_s, and η) (note that Θ_w is not required to calculate vertical percolation), using the work presented in this study, it is possible to estimate all of these from just two soil texture parameters (% sand and % silt).

Four of the seven parameters (α, n, K_s, and η) are associated with the *van Genuchten* [1980] functions for effective saturation and hydraulic conductivity of unsaturated soils. These can be obtained for a given soil texture directly from the ROSETTA model [*Schaap et al*., 2001]. Relationships between the other four parameters (the infiltration capacity, q_{ic}, the storage capacity available for plant uptake, Θ_{pu}, the residence time of the linear reservoir, T_r, and the water level at which plant wilting occurs, Θ_w) and soil texture are obtained by calibrating the SMAP model to vertical percolation and runoff data obtained from a sequence of Richards' equation (RE) models.

The RE model used for the calibration exercise comprise of a 3 m one-dimensional homogenous single porosity soil column with an exponentially distributed plant root distribution spanning the top 1 m. The model is run for 231 different soil textures using 36 years of daily rainfall data and monthly potential evapotranspiration data from a southern English catchment. Following calibration, the new SMAP is found to predict storage levels and vertical percolation rates from the RE model with *Nash and Sutcliffe* [1970] efficiencies greater than 0.7 and 0.65, respectively, for all soil textures.

Results from the 231 numerical simulations are also found to be qualitatively consistent with intuitive ideas concerning soil texture and soil moisture dynamics. Vertical percolation rates are found to be highest in sandy soils. Sandy soils are found to provide less water for evapotranspiration. Surface runoff is found to be more important in soils with high clay content.

The calibration has been carried out using meteorological data for a UK maritime climate. The advantage of such a data set is that it contains months of high rainfall and low evapotranspiration, months of low rainfall

and high evapotranspiration, months of high rainfall and high evapotranspiration, and months of low rainfall and low evapotranspiration. Therefore, the calibration should hold well for other temperate or tropical climates. However, the meteorological data set does not include years containing zero or near-zero rainfall. It would be interesting to repeat the calibration for a much drier climate.

In the current study, the main focus is on how to parameterize the SMAP model for different soil textures. During the study, the distribution of plant root density and the depth of the soil layer were held constant. Another interesting study could look at how calibrated SMAP parameters vary with soil depth and plant roots depth.

The calibration study involved using the *van Genuchten* [1980] functions for moisture content and hydraulic conductivity, which is suitable for single porous media. However, these could be replaced with an equivalent composite model for dual porosity media [*Peters and Klavetter*, 1988] in both the RE model and the SMAP model to include for the presence of macroporous and/or fracture flow in future studies.

Acknowledgments
The views expressed in this article are those of the authors and do not necessarily represent the views of, and should not be attributed to, AMEC. The authors are also grateful for the useful comments and recommendations made by the Editors and Reviewers at Water Resources Research. Data used in the manuscript can be obtained by directly contacting the corresponding author.

References

Allen, R. G., L. S. Pereira, D. Raes, and M. Smith (1998), Crop evapotranspiration-guidelines for computing crop water requirements, *FAO Irrig. Drain. Pap. 56*, Food and Agriculture Organization, Rome.

Assefa, K. A., and A. D. Woodbury (2013), Transient, spatially varied groundwater recharge modeling, *Water Resour. Res.*, *49*, 4593–4606, doi: 10.1002/wrcr.20332.

Aston, A. R., and F. X. Dunin (1977), An empirical model for drainage from soil under rain fed conditions, *Aust. J. Soil Res.*, *15*, 205–210.

Best, M. J., et al. (2011), The Joint UK Land Environment Simulator (JULES), model description-Part 1: Energy and water fluxes, *Geosci. Model Dev.*, *4*, 677–699.

Beven, K., and J. Freer (2001), Equifinality, data assimilation, and uncertainty estimation in mechanistic modelling of complex environmental systems using the GLUE methodology, *J. Hydrol.*, *249*, 11–29.

Black, T. A., W. R. Gardner, and G. W. Thurtell (1969), The prediction of evaporation, drainage, and soil water storage for a bare soil, *Soil Sci. Soc. Am. J.*, *33*, 655–660.

Bradford, R. B., R. Ragab, S. M. Crooks, F. Bouraoui, and E. Peters (2002), Simplicity versus complexity in modelling groundwater recharge in Chalk catchments, *Hydrol. Earth Syst. Sci. Discuss.*, *6*, 927–937.

Carrera-Hernandez, J. J., B. D. Smerdon, and C. A. Mendoza (2012), Estimating groundwater recharge through unsaturated flow modelling: Sensitivity to boundary conditions and vertical discretization, *J. Hydrol.*, *452*, 90–101.

Chapman, T. G., and R. W. Malone (2002), Comparison of models for estimation of groundwater recharge, using data from a deep weighing lysimeter, *Math. Comput. Simul.*, *59*, 3–17.

Croke, B. F., and A. J. Jakeman (2004), A catchment moisture deficit module for the IHACRES rainfall-runoff model, *Environ. Modell. Software*, *19*, 1–5.

Cox, P. M., R. A. Betts, C. B. Bunton, R. L. H. Essery, P. R. Rowntree, and J. Smith (1999), The impact of new land surface physics on the GCM simulation of climate and climate sensitivity, *Clim. Dyn.*, *15*, 183–203.

de Rosnay, P., M. Bruen, and J. Polcher (2000), Sensitivity of surface fluxes to the number of layers in the soil model used in GCMs, *Geophys. Res. Lett.*, *27*, 3329–3332.

Evans, J. P., and A. J. Jakeman (1998), Development of a simple, catchment-scale, rainfall-evapotranspiration-runoff model, *Environ. Modell. Software*, *13*, 385–393.

Feddes, R. A., P. Kowalik, K. Kolinska–Malinka, and H. Zaradny (1976), Simulation of field water uptake by plants using a soil water dependent root extraction function, *J. Hydrol.*, *31*, 13–26.

Finch, J. W. (2001), Estimating change in direct groundwater recharge using a spatially distributed soil water balance model, *Q. J. Eng. Geol. Hydrogeol.*, *34*, 71–83.

Grindley, F. (1967), Estimation of soil moisture deficits, *Meteorol. Mag.*, *96*, 97–108.

Heathcote, J. A., R. T. Lewis, and R. W. N. Soley (2004), Rainfall routing to runoff and recharge for regional groundwater resource models, *Q. J. Eng. Geol. Hydrogeol.*, *37*, 113–130.

Hough, M. (1995), The Meteorological Office Rainfall and Evaporation Calculation System: MORECS Version 2.0, *Hydrol. Memo.45*, Meteorol. Off., U. K.

Ireson, A. M., and A. P. Butler (2013), A critical assessment of simple recharge models: Application to the UK Chalk, *Hydrol. Earth Syst. Sci.*, *17*, 2083–2096.

Ireson, A. M., S. A. Mathias, H. S. Wheater, A. P. Butler, and J. Finch (2009), A model for flow in the chalk unsaturated zone incorporating progressive weathering, *J. Hydrol.*, *365*, 244–260.

Jones, S. B. (1983), The estimation of catchment average point rainfall profiles, *Rep. 87*, Inst. Hydrol., Wallingford, U. K.

Marthews, T. R., C. A. Quesada, D. R. Galbraith, Y. Malhi, C. E. Mullins, M. G. Hodnett, and I. Dharssi (2014), High-resolution hydraulic parameter maps for surface soils in tropical South America, *Geosci. Model Dev.*, *7*, 711–723.

Mathias, S. A., A. P. Butler, B. M. Jackson, and H. S. Wheater (2006), Transient simulations of flow and transport in the Chalk unsaturated zone, *J. Hydrol.*, *330*, 10–28.

Mathias, S. A., A. P. Butler, and H. S. Wheater (2008), Modelling radioiodine transport across a capillary fringe, *J. Environ. Radioact.*, *99*, 716–729.

McIntyre, N., H. Lee, H. Wheater, A. Young, and T. Wagener (2005), Ensemble predictions of runoff in ungauged catchments, *Water Resour. Res.*, *41*, W12434, doi:10.1029/2005WR004289.

Miegel, K., K. Bohne, and G. Wessolek (2013), Prediction of long-term groundwater recharge by using hydropedotransfer functions, *Int. Agrophys.*, *27*, 31–37.

Nash, J., and J. V. Sutcliffe (1970), River flow forecasting through conceptual models part IA discussion of principles, *J. Hydrol.*, *10*, 282–290.

Peters, R., and E. A. Klavetter (1988), A continuum model for water movement in an unsaturated fractured rock mass, *Water Resour. Res.*, *24*, 416–430.
Quinn, S. A., D. Liss, D. Johnson, J. J. Van Wonderen, and T. Power (2012), Recharge estimation methodologies employed by the Environment Agency of England and Wales for the purposes of regional groundwater resource modelling, *Geol. Soc. Spec. Publ.*, *364*, 65–83.
Ragab, R., J. Finch, and R. Harding (1997), Estimation of groundwater recharge to chalk and sandstone aquifers using simple soil models, *J. Hydrol.*, *190*, 19–41.
Rushton, K. R. (2005), Estimating recharge for British aquifers, *Water Environ. J.*, *19*, 115–124.
Schaap, M. G., F. J. Leij, and M. T. van Genuchten (2001), Rosetta: A computer program for estimating soil hydraulic parameters with hierarchical pedotransfer functions, *J. Hydrol.*, *251*, 163–176.
Shampine, L. F., and M. W. Reichelt (1997), The matlab ode suite, *SIAM J. Sci. Comput.*, *18*, 1–22.
Simunek, J., M. T. van Genuchten, and M. Sejna (2008), Development and applications of the HYDRUS and STANMOD software packages and related codes, *Vadose Zone J.*, *7*, 587–600.
Smith, R. N. B., E. M. Blyth, J. W. Finch, S. Goodchild, R. L. Hall, and S. Madry (2006), Soil state and surface hydrology diagnosis based on MOSES in the Met Office Nimrod nowcasting system, *Meteorol. Appl.*, *13*, 89–109.
Sorensen, J. P. R., J. W. Finch, A. M. Ireson, and C. R. Jackson (2014), Comparison of varied complexity models simulating recharge at the field scale, *Hydrol. Processes*, *28*, 2091–2102.
Tocci, M. D., C. T. Kelley, and C. T. Miller (1997), Accurate and economical solution of the pressure-head form of Richards' equation by the method of lines, *Adv. Water Resour.*, *20*, 1–14.
Twarakavi, N. K. C., M. Sakai, and J. Simunek (2009), An objective analysis of the dynamic nature of field capacity, *Water Resour. Res.*, *45*, W10410, doi:10.1029/2009WR007944.
van Genuchten, M. T. (1980), A closed-form equation for predicting the hydraulic conductivity of unsaturated soils, *Soil Sci. Soc. Am. J.*, *44*, 892–898.
Wagener, T., D. P. Boyle, M. J. Lees, H. S. Wheater, H. V. Gupta, and S. Sorooshian (1999), A framework for development and application of hydrological models, *Hydrol. Earth Syst. Sci.*, *5*, 13–26.
Wagener, T., N. McIntyre, M. J. Lees, H. S. Wheater, and H. V. Gupta (2003), Towards reduced uncertainty in conceptual rainfall-runoff modelling: Dynamic identifiability analysis, *Hydrol. Processes*, *17*, 455–476.
Wellings, S. R., and J. P. Bell (1980), Movement of water and nitrate in the unsaturated zone of Upper Chalk near Winchester, Hants., England, *J. Hydrol.*, *48*, 119–136.
Young, A. (2000), Regionalizing a daily rainfall-runoff model within the United Kingdom, PhD thesis, Univ. of Southampton, Southampton, U. K.
Young, A. (2006), Stream flow simulation within UK ungauged catchments using a daily rainfall-runoff model, *J. Hydrol.*, *320*, 155–172.